GEORGIA INSTITUTE OF TECHNOLOGY
OFFICE OF CONTRACT ADMINISTRATION
SPONSORED PROJECT INITIATION

GIS

Date: 11/1/77

Project Title: "The Effect of Microstructural Features on Corrosion on Fatigue of High Strength Aluminum Alloys."

Project No: E-19-659

Project Director: Dr. E. A. Starke

Sponsor: U.S. Air Force of Scientific Research; Bolling AFB, D. C.

Agreement Period: From 1/1/78 Until 12/31/78

Type Agreement: AFOSR-
Grant No. 78-3471

Amount: $65,000 (AFOSR Funds - E-19-659)
17,159 (GIT Funds - E-19-339)
$82,159 TOTAL

Reports Required: Final Technical Report, Interim Technical Reports

Sponsor Contact Person (s):

Technical Matters

Alan H. Rosentein
U.S. Air Force
Office of Scientific Research
Building 410
Bolling AFB, D. C. 20332

Contractual Matters
(thru OCA)

Joan O. Marshall, Contracting Officer
U.S. Air Force
Office of Scientific Research
Building 410
Bolling AFB, D. C. 20332

Defense Priority Rating: N/A

Assigned to: Chemical Engineering (School/Laboratory)

COPIES TO:

- Project Director
- Division Chief (EES)
- School/Laboratory Director
- Dean/Director–EES
- Accounting Office
- Procurement Office
- Security Coordinator (OCA)
- Reports Coordinator (OCA)
- Library, Technical Reports Section
- EES Information Office
- EES Reports & Procedures
- Project File (OCA)
- Project Code (GTRI)
- Other

CA–3 (3/76)

GEORGIA INSTITUTE OF TECHNOLOGY
OFFICE OF CONTRACT ADMINISTRATION

SPONSORED PROJECT TERMINATION

Date: 2/5/79

Project Title: *The Effect of Microstructural Features on Corrosion of Fatigue of High Strength Aluminum Alloys*

Project No: *E-19-659*

Project Director: *Dr. E. A. Starke, Jr.*

Sponsor: *Air Force Office of Scientific Research*

Effective Termination Date: *12/31/78* *(Continued under E-19-674)*

Clearance of Accounting Charges: *12/31/78*

Grant/Contract Closeout Actions Remaining:

- _ Final Invoice and Closing Documents
- _ Final Fiscal Report
- x ~~Final~~ Report of Inventions *(Interim)*
- _ Govt. Property Inventory & Related Certificate
- _ Classified Material Certificate
- _ Other _____

Assigned to: *Chemical Engineering* (School/Laboratory)

COPIES TO:

Project Director
Division Chief (EES)
School/Laboratory Director
Dean/Director–EES
Accounting Office
Procurement Office
Sponsored Coordinator (OCA) ✓
Reports Coordinator (OCA)
Library, Technical Reports Section
Office of Computing Services
Director, Physical Plant
EES Information Office
Project File (OCA)
Project Code (GTRI)
Other _____

CA–4 (3/76)

SECURITY CLASSIFICATION OF THIS PAGE *(When Data Entered)*

REPORT DOCUMENTATION PAGE		READ INSTRUCTIONS BEFORE COMPLETING FORM
1. REPORT NUMBER	2. GOVT ACCESSION NO.	3. RECIPIENT'S CATALOG NUMBER
4. TITLE *(and Subtitle)* The Effect of Copper Content & Degree of Recrystallization on the Fatigue Resistance of 7XXX-Type Aluminum Alloys. Part I: Low Cycle Corrosion Fatigue		5. TYPE OF REPORT & PERIOD COVERED Scientific report 1/1/78-12/31/78 6. PERFORMING ORG. REPORT NUMBER
7. AUTHOR(s) Fu-Shiong Lin and E. A. Starke, Jr.		8. CONTRACT OR GRANT NUMBER(s) AFOSR 78-3471
9. PERFORMING ORGANIZATION NAME AND ADDRESS Fracture and Fatigue Research Laboratory Georgia Institute of Technology Atlanta, Georgia 30332		10. PROGRAM ELEMENT, PROJECT, TASK AREA & WORK UNIT NUMBERS
11. CONTROLLING OFFICE NAME AND ADDRESS Electronic & Solid State Sciences Air Force Office of Scientific Research Bolling AFB, Building 410 Washington, DC 20332		12. REPORT DATE 1/1/78-12/31/78 13. NUMBER OF PAGES 46
14. MONITORING AGENCY NAME & ADDRESS *(if different from Controlling Office)*		15. SECURITY CLASS. *(of this report)* Unclassified 15a. DECLASSIFICATION/DOWNGRADING SCHEDULE
16. DISTRIBUTION STATEMENT *(of this Report)* unlimited		
17. DISTRIBUTION STATEMENT *(of the abstract entered in Block 20, if different from Report)*		
18. SUPPLEMENTARY NOTES		
19. KEY WORDS *(Continue on reverse side if necessary and identify by block number)* 7XXX-Type Aluminum fatigue age hardening corrosion		
20. ABSTRACT *(Continue on reverse side if necessary and identify by block number)* The effect of copper content (from 0.01 to 2.1%) and degree of recrystallization (DR from 5 to 45%) on the corrosion fatigue behavior of four Al-6Zn-2Mg-xCu-T651 alloys was investigated. The cyclic strain resistance was found to increase with copper content and decrease with DR regardless of the test environment. This trend is more pronounced in aggressive environments. The improved fatigue resistance is attributed to the increased homogeneity of slip as the copper content is increased and the DR is decreased. The environmental sensitivity, which increases with decreasing copper content, is dependent on slip behavior.		

DD FORM 1 JAN 73 1473 EDITION OF 1 NOV 65 IS OBSOLETE

SECURITY CLASSIFICATION OF THIS PAGE *(When Data Entered)*

For alloys tested in distilled water, hydrogen embrittlement is believed to be the major factor controlling the low cycle corrosion fatigue. For tests conducted in a 3.5% NaCl solution, hydrogen embrittlement still plays as important role, but the preferential dissolution and/or adsorption process may also have a detrimental effect.

ACCEPTED FOR PUBLICATION IN
MATERIAL SCIENCE & ENGINEERING

THE EFFECT OF COPPER CONTENT AND DEGREE OF RECRYSTALLIZATION ON THE FATIGUE RESISTANCE OF 7XXX-TYPE ALUMINUM ALLOYS*

PART I. LOW CYCLE CORROSION FATIGUE

Fu-Shiong Lin and E. A. Starke, Jr.
Fracture and Fatigue Research Laboratory
Georgia Institute of Technology
Atlanta, Georgia 30332

Abstract

The effect of copper content (from 0.01 to 2.1%) and degree of recrystallization (DR from 5 to 45%) on the corrosion fatigue behavior of four Al-6Zn-2Mg-xCu-T651 alloys was investigated. The cyclic strain resistance was found to increase with copper content and decrease with DR regardless of the test environment. This trend is more pronounced in aggressive environments. The improved fatigue resistance is attributed to the increased homogeneity of slip as the copper content is increased and the DR is decreased. The environmental sensitivity, which increases with decreasing copper content, is dependent on slip behavior. For alloys tested in distilled water, hydrogen embrittlement is believed to be the major factor controlling the low cycle corrosion fatigue. For tests conducted in a 3.5% NaCl solution, hydrogen embrittlement still plays an important role, but the preferential dissolution and/or adsorption process may also have a detrimental effect.

* This research represents a portion of the thesis submitted by Fu-Shiong Lin to the Georgia Institute of Technology, in partial fulfillment of the requirements for the degree of Doctor of Philosophy in the School of Chemical Engineering and Metallurgy.

INTRODUCTION

The use of fail-safe and safe-life design philosophies has resulted in increased research activity directed towards understanding the corrosion fatigue behavior of 7XXX aluminum alloys important to the aircraft industry. Conventional studies of such variables as alloy chemistry[1,2], aging treatment[3-6], grain structure,[7] inclusion content[8,9], and thermomechanical processing[10-12] have identified some parameters important to fatigue resistance. However, numerous inconsistencies exist among these investigations. Large discrepancies may result from the failure to characterize some microstructural parameters such as grain size, inclusion content, degree of recrystallization (DR), etc. Although the effects of these parameters on fatigue properties have not been completely established, it is believed that they do have an influence.

This research is designed to sort out the contribution of various microstructural parameters on the corrosion fatigue behavior of high strength 7XXX-type alloys. Four Al-6Zn-2Mg-xCu type aluminum alloys with almost identical microstructures (e.g., DR, grain size and subgrain size) were chosen to study the effect of copper content on fatigue properties. Each alloy was also processed to produce different DR in order to investigate the effect of that microstructural feature on fatigue behavior. PART I deals with the effect of copper content and DR on the low cycle fatigue (LCF) behavior in the presence of dry air, distilled water and a 3.5% NaCl solution. PART II deals with the effect of these two parameters on the fatigue crack growth in these environments.

EXPERIMENTAL PROCEDURES

The chemical compositions of the four 7XXX-type alloys are shown in Table I. An attempt was made to produce four different DR for each alloy by rolling them at different temperatures, but with the same percentage of reduction. The

maximum DR was obtained by rolling the plates at lower temperatures and at a higher percentage of reduction than those of low DR. The manufacturing processes were conducted in two stages as follows. Initial procedure: 5.6 cm thick plates of all alloys were rolled to 1.9 cm thickness, using identical procedures. These consisted of homogenization at 480°C for 12 hours, an air cool to 400°C, and then reduction to final thickness in six passes. The percentage of reduction for each pass was 18.2, 11.1, 12.5, 14.3, 16.7 and 25.0%, respectively, and the plates were reheated to 400°C between passes. Final procedure: Four different rolling schedules were followed to produce a different DR for each alloy. They are as follows for the 1.9 cm plates:

No. 1: The plates were rolled to 0.64 cm in two passes. The percentage of reduction for each pass being 40.0 and 44.4%, respectively, with a 400°C reheat before each pass.

No. 2: The same as No. 1 except for a reheat temperature of 370°C.

No. 3: The same as No. 1 except for a reheat temperature of 340°C.

No. 4: The plates were reheated to a temperature of 260°C, and then rolled directly to the final thickness of 0.64 cm (66.7% reduction).

Finally the alloys were solutionized, stretched 1.5%, and aged for 24 hours at a temperature of 120°C. They may be considered to be in a maximum strength T651 temper. All were prepared at the Alcoa Technical Center, Pa.

Optical microscopy was used to determine the DR after etching the specimens. Figure 1a shows a partially recrystallized structure in which the dark areas are unrecrystallized grains. Figure 1b shows an unrecrystallized structure etched to bring out the subgrain boundaries. The method employed for determination of DR (i.e., volume percent recrystallized) was the point counting analysis described by Hilliard[13]. Because the DR varies significantly with distance from the plate surfaces, the magnitude of DR for the entire plate was determined by averaging

measurements taken from a vertical section through the thickness. Both L-S (longitudinal-short transverse) and T-S (long transverse-short transverse) sections were used for the determination. Optical microscopy was also used to observe crack initiation on the LCF samples.

The mean intercept length (MIL) and the standard diviation (S) of the sub-grains in the unrecrystallized grains of the various aluminum alloys was determined from transmission electron micrographs. Thin foils were systematically cut from different depths in the plate in L-S sections. The MIL was measured in the longitudinal direction and expressed as the nearest integral number of microns. In order to observe the changes of microstructure due to cyclic loading, thin foils were cut from the LCF test samples, 1-3 mm below the fracture surface and prepared for TEM by a dimpling technique using a 25% HNO_3-methanol solution. The foils were examined in a JEOL-JEM-100C electron microscope operating at 100 KV.

Specimens of each alloy with the minimum DR were used for studying the effect of copper content on the LCF properties since this condition produced the same grain structure for all alloys. Both 1.6 and 2.1% Cu alloys, each with two different DR, were chosen for investigating the effect of DR on the LCF behavior since they showed the largest difference of the four alloys. The test samples were machined with the tensile axes perpendicular to the rolling direction of the plate. The samples were cylindrical with a gage section approximately 5.0 mm long by 3.0 mm in diameter. They were hand-polished with 320 and 600 grit emery paper, then with polishing cloths impregnated with 6 μm and 1 μm diamond paste. Some of the samples were electropolished for surface observations after the tests.

Tension-compression LCF tests were performed in an Instron Testing Machine at a cross head speed of 2 mm/min. The strain was measured with a 10mm extensometer

clamped to struts rigidly fixed to the grips. A Wood's metal reservoir was used to insure proper alignment of the sample with respect to the loading axis. Tests were conducted either in dry air (3 ppm max. H_2O content), distilled water or a 3.5% NaCl solution. For the two aqueous tests a soft cup 2 inches in diameter was sealed to the sample which was completely submerged in the solution.

EXPERIMENTAL RESULTS AND DISCUSSION

Microstructural Characteristics

The DR (in volume percent recrystallized) for the alloys studied are presented in Table 2. The unrecrystallized, large grains (about 1100 μm) for the four alloys at these DR (3, 3, 5 and 6%) are essentially identical because they were rolled under the same schedule. Since the recrystallized grains represented a small volume fraction and since their size varied from 10 μm to 370 μm, the determination of an average grain size was not warranted.

The MIL and S of the subgrains in the unrecrystallized grains for the various alloys and DR are given in Table 2. The small difference in MIL and S between the various alloys with low DR is not likely to significantly affect the LCF behavior. The MIL is remarkably different between an alloy with low DR and the same alloy with high DR. The initial subgrain size due to hot rolling is strictly dependent upon the magnitude of deformation with the size decreasing with increasing deformation.[14] Thus, an alloy with high DR contained smaller subgrains since it was hot rolled to a 22% greater reduction than the same alloy with low DR. The presence of very fine Al_3Zr particles in these alloys helps to stablilize the subgrain structure even during solutionizing at high temperature.

TEM was used to examine the precipitation features on subgrain and high-angle-grain boundaries of all the alloys. No significant difference in precipitate distribution was found between these two different types of boundaries for this aging treatment and for the four alloys. Both low angle and high angle boundaries were covered with small rod shaped, η' as shown in Figure 2. Since the aging temperature was below T_c[15], no significant PFZ was present.

Monotonic Mechanical Properties

The monotonic mechanical properties are presented in Table 3. The yield strength, tensile strength, ductility and strain hardening exponent (n), in genreral, increase with increasing copper content. This is especially true for the yield strength and ductility. This trend can be attributed to the fact that the addition of copper in Al-Zn-Mg alloys not only increases the volume fraction of strengthening precipitates[4,16], but also increases the number of partially coherent and incoherent precipitates[4] and thus the homogeneity of deformation. The monotonic strength parameters are not significantly affected by the changes of DR since these properties are controlled by the strengthening precipitates and not grain structure.

Cyclic Stress Strain Response

The cyclic hardening and softening curves exhibited significant hardening in the first few cycles and then reached a saturated condition. Afterwards, cyclic softening occurred in most samples--especially for tests conducted in dry

air. For instance, specimens of 0.01, 1.0 and 1.6% Cu alloys displayed cyclic softening in dry air, but only a few samples displayed cyclic softening in distilled water or in a 3.5% NaCl solution, Figures 3 to 6. However, cyclic softening was exhibited by samples of the 2.1% Cu alloy for all test environments, Figures 7 and 8. It is very important to note that if a sample exhibits cyclic softening, the softening is clearly identified by a gradual decrease of both tensile and compressive stress during cyclic-straining. The DR had little or no effect on the cyclic stress strain response, Figures 5 through 8.

The absence of cyclic softening for the low copper content alloys ($\leq$1.6% Cu) tested in distilled water or a 3.5% NaCl solution is not due to the environmental effect on the cyclic softening processes, but due to environment induced cracking prior to softening. This can be seen by comparing the number of cycles for softening in dry air with that for failure in distilled water or in a 3.5% NaCl solution. For example, in the 0.01% Cu alloy, the number of cycles for softening is 25 cycles ($\Delta\varepsilon_p/2$ = 1.58%) in dry air, Figure 3, but a sample of an identical alloy failed at 15 cycles ($\Delta\varepsilon_p/2$ - 1.43%) in distilled water. Thus, cyclic softening was not found in the latter environment. On the other hand, the fatigue life of the 2.1% Cu alloy was not significantly affected by distilled water, and hence, cyclic softening was observed for the samples tested in both dry air and distilled water, Figures 7 and 8. Consequently, cyclic softening observed in this study is a mechanical and not an environmental effect.

Cyclic softening has been observed in a high purity ITMT 7075 alloy[17] and attributed to the rearrangement of dislocations introduced by the final deformation. However, cyclic softening is normally thought to be associated with precipitate resolution during cyclic-loading, aging inhomogeneities[18-19], or a disordering mechanism.[20] If these mechanisms were operative the resistance to cyclic softening should logically increase with increasing copper content since the

extent of homogeneity of deformation and the degree of homogeneity of precipitate distribution are increased as copper content increases. The test results showed, however, that the number of cycles for softening does not systematically increase with increasing copper content. For example, for the 0.01 and 1.6% Cu alloys cyclic-strained in dry air at $\Delta\varepsilon_p/2$ = 1.58 and 1.52% respectively, the 0.01% Cu alloy needed 20 cycles for softening while the 1.6% Cu alloy required 10 cycles, Figures 3 and 5. Also for low strain amplitude tests in dry air the 1.0% Cu alloy needed 130 cycles ($\Delta\varepsilon_p/2$ = 0.59%) for softening which was more than the 50 cycles required for the 2.1% Cu alloy ($\Delta\varepsilon_p/2$ = 0.53%), Figures 5 and 9.

Stoltz and Pelloux[21] have shown that 7XXX aluminum alloys heat treated to contain easily shearable precipitates exhibit a small Bauschinger stress while alloys with nonshearable precipitates show a larger stress. Therefore, Bauschinger stress measurements may provide evidence of dislocation shearing of coherent precipitates and dislocation looping of incoherent precipitates for the 7XXX alloys of our study. The effect of copper content on the Bauschinger stress is shown in Figure 9. The stress increases slightly as copper content changes from 0.01 to 1.6%, especially for total strains smaller than 4.5%; whereas the stress increases tremendously for the 2.1% Cu alloy. This suggests that the alloys with copper contents $\leq$ 1.6% contain shearable precipitates and the 2.1% Cu alloy contains nonshearable precipitates. Grain and/or subgrain boundaries do not greatly affect the Bauschinger stress since similar values were obtained for the same alloy with different DR. These measurements would indicate that if precipitate shearing is the only cause for the observed cyclic softening, the extent of softening should decrease with increasing copper content.

Extensive TEM examination was made of thin foils cut from the LCF test samples in order to determine the softening mechanism. In general, the appearance of the microstructures after cyclic deformation was similar for the low copper content

alloys (0.1 to 1.6% Cu), i.e., predominately uniform despite the magnitude of plastic strain. The uniformity of plastic strain, when compared to our previous studies,[4] is most likely associated with the small subgrain size and the presence of Al_3Zr dispersoids. Some persistent slip bands were found, however, in the lower copper content alloys with the frequency of occurrence decreasing with increasing copper content. It is important to note that although cyclic softening was observed for the 2.1% Cu alloy, similar slip bands were not observed regardless of plastic strain and DR. Figure 10 (a-c) shows typical examples of slip band features for the lower copper content alloys. Presumably, in addition to softening on the localized slip bands[18,27], other factors may be involved in the cyclic softening processes, at least in this study. The occurrence of extensive grain boundary cracking may play some part in the softening processes since the microcracks will reduce the strength and may also induce dislocation egression. This explanation is in agreement with the findings of Calabrese and Laird[20] who indicated that crack initiation takes place at grain boundaries for alloys containing nonshearable precipitates. Our study showed that the 2.1% Cu alloy is more susceptible to cyclic softening, and this may be due to grain boundary cracking associated with more incoherent precipitates than present in the other alloys.

The data of Figures 3-8 can be used to determine the cyclic stress strain curves and the cyclic strain hardening exponent, n'. These curves and the values of n' for the different copper content alloys are shown in Figure 11. The values of n' increase with increasing copper content in general agreement with the mechanism of work hardening for precipitation hardenable alloys.[22] The lower copper content alloys contain more easily shearable precipitates resulting in lower values of n'. The higher copper content alloys contain partially coherent and incoherent precipitates which are looped by dislocations, resulting in

higher values of n'. Note that for the 1.6 and 2.1% Cu alloys, the lower DR exhibits a higher value of n' than found for the same alloy with high DR. This suggests that the subgrains in the unrecrystallized grains increase the cyclic hardening behavior by increasing the number of slip interactions.

The Effect of Copper Content on LCF Life

The effect of copper on the LCF life in the various environments is shown in Figure 12(a-c). The values of important parameters derived from these plots are presented in Table 4. It is evident that the cyclic strain resistance of these 7XXX-type aluminum alloys generally increases with increasing copper content, regardless of the test environment. This trend becomes much more noticeable when the tests are conducted in distilled water or a 3.5% NaCl solution. The difference in cyclic strain resistance for the four alloys decreases at high plastic strain amplitudes, especially for tests conducted in dry air.

As noted in the Introduction, the alloys chosen for investigating the effect of copper content on the LCF behavior had almost identical microstructures, e.g., the DR, the unrecrystallized grain size and subgrain size. Therefore, the only significant parameter to affect the LCF properties appears to be the copper content. Copper participates in the precipitation process during aging and changes the character of the precipitates.[4,16,23,24] As a result, copper alters the type of interactions between precipitates and dislocations. The more shearable precipitates of the lower copper content alloys lead to coarse planar slip on a macroscopic scale, Figure 13a. In contrast, the 2.1% Cu alloy developed diffuse wavy slip bands, Figure 13b. Planar slip may increase the reversibility of slip and thus improve the LCF resistance for some low SFE materials[25,26], however, in age-hardenable alloys planar slip can cause softening in the slip bands[18,27], resulting in strain localization. This leads to early crack initiation by slip band decohesion, especially in corrosive environments, since localized strain

concentrations intensify metal-environment interactions. For the high copper content alloy such as 2.1% Cu, not only do dislocations shear coherent and partially coherent precipitates, but they also loop the more numerous incoherent precipitates. The latter deformation mechanism reduces the slip reversibility, but results in a high degree of homogeneity of deformation. Optical observations of the surfaces of fatigue specimens made from alloys with low copper contents also showed that cracks initiated in the slip bands and then propagated along these preferable paths, as shown in Figure 14.

A break in the Coffin-Manson plot was found for plastic strain amplitudes greater than 1.2% for most alloys, regardless of the test environment, Figure 13. The occurrence of a break at high plastic strain amplitude has been explained by several investigators.[4,5,28,29] One suggestion is that the break is associated with a change in the crack propagation mode from intergranular to transgranular.[22] Our observations indicate that this is not the case although a transition from a ductile to a more brittle fracture mode cannot be ruled out, Figure 16. The break has also been suggested to be due to a change in the deformation processes as a function of plastic strain amplitude.[4] For the range of plastic strain amplitudes employed in this study, cell structures due to cyclic-loading were not found in thin foils by TEM; thus, this mechanism does not apply here. Another suggestion is that the break is due to a change from localized slip bands to homogeneous slip as a function of plastic strain amplitude.[5,29] Changes in the homogeneity of deformation were observed on a macroscopic scale, and the break may be due to the difference in frequency of occurrence and to the intensity of slip bands at low and high strain amplitudes. However, quantitative correlation between these features and the break in the Coffin-Manson plot was not established. Therefore, no unequivocal explanation for the discontinuity was derived from this study.

Effect of Environment on the LCF Life

The LCF resistance of aluminum alloys was considerably affected by the presence of distilled water or a 3.5% NaCl solution as shown in Figure 16. This trend becomes much more noticeable as the copper content decreases. For example, the ratio of the fatigue life of the aluminum alloy in dry air to that in distilled water (for $\Delta\varepsilon_p/2 = 1.0\%$) is 4.0, 2.0, 1.7 and 1.2, for 0.01, 1.0, 1.6 and 2.1% Cu alloys, respectively. The environmental effect on the appearance of the fatigue fracture surfaces are shown in Figures 17 and 18 for the lowest and highest copper content alloys. For the 0.01% Cu alloy, a few ductile striations were developed on the fracture surface within the stable fracture region as shown in micrograph (a) of Figure 17, but a considerable amount of area is relatively featureless. This indicates that only a few slip systems were involved in the crack propagation. For tests conducted in distilled water, wide steps and straight cleavage-like markings running normal to the steps are observed, micrograph (b), indicating that the direction of crack propagation was changed for each step. The cleavage-like markings are indicative of brittle fracture.

The fracture surface appearance in the overload fracture region exhibits dimple patterns combined with some secondary cracking along the grain boundaries for all samples tested in the three environments. The fracture surface features and the LCF lives of samples tested in a 3.5% NaCl solution and distilled water are similar. For samples of the 2.1% Cu alloy tested in dry air, the fracture surface in the stable fracture region exhibits the regular ductile striations, and numerous plateaus and ridges as shown in micrograph (a) of Figure 18. These features are indicative of ductile fatigue fracture and many slip systems are involved in the crack propagation. In contrast to the 0.01% Cu alloy, the fracture surface features for the 2.1% Cu alloy tested in distilled water still exhibits the ductile striations combined with local featureless areas, as shown in micrograph (b). The amount of featureless area is larger than that observed

in dry air. The fracture surface in the overload fracture region displays dimple patterns regardless of the test environment. These observations support the previous conclusion that an increase of copper content in 7XXX-type aluminum alloys decreases environmental sensitivity.

Several mechanisms[30-44] of corrosion fatigue have been proposed to explain the decrease of fatigue resistance in the presence of corrosive environments. These include anodic dissolution, adsorption, an oxide film effect and hydrogen embrittlement. When the LCF sample is tested in distilled water, the major electrochemical reactions are hydrogen evolution and oxide formation. However, oxide formation also occurs in dry air. Lowering of the elastic modulus of the oxide layer by water adsorption is considered unlikely to have a large detrimental effect.[35] Our results indicate that the decrease in cyclic strain resistance of aluminum alloys in distilled water is primarily due to hydrogen embrittlement. Recent results obtained by other investigators[45] support this interpretation. They suggest that the low diffusivity of hydrogen is counterbalanced by the fact that hydrogen need only be present at the specimen surface for crack initiation and in the plastic zone of growing cracks for propagation. The mechanism possibly involves the production of hydrogen atoms at clean surfaces exposed by slip or at the crack tip during cyclic-loading, and subsequent diffusion of hydrogen atoms into the metal. The exact mechanism of hydrogen embrittlement in aluminum alloys is still unknown, but it may be due to the combined action of high pressure of hydrogen, a decrease of plasticity and a reduction of the cohesive strength of the lattice by adsorbed hydrogen.

In a 3.5% NaCl solution, the cyclic strain resistance is further decreased. For this case, hydrogen embrittlement may still play an important role but anodic dissolution at the slip bands may also accelerate crack initiation[41-44] and crack propagation. Another possible contribution to corrosion fatigue in a 3.5%

NaCl solution may be an adsorption process[44,46] which lowers the surface energy and changes the fracture process.

Although the mechanism of corrosion fatigue is not understood exactly, it is well known that change of slip behavior can affect the susceptibility to corrosion fatigue. The present study clearly shows that the environmental sensitivity of 7XXX-type aluminum alloys can be suppressed by additions of copper. Ample results of the cyclic deformation characteristics for the alloys of this study combined with the recent suggestions of the mechanism of hydrogen embrittlement[47,48] can be used to interpret this phenomenon. An increase in copper content increases the homogeneity of deformation, resulting in a decrease of the metal-environment interactions. For the low copper alloys, especially for the 0.01% Cu alloy, dislocation shearing of coherent precipitates results in planar slip. More hydrogen atoms can be transported by the dislocations moving in the localized slip bands, resulting in localized regions of high hydrogen concentration.

Effect of DR on the LCF Life

The effect of DR on the LCF behavior of the 1.6 (DR = 5% and 30%) and 2.1% (DR = 6% and 45%) Cu alloys is shown in Figure 16 (c and d), plotted as $\Delta\varepsilon_p/2$ vs. $2N_f$. It is apparent from these curves that the cyclic strain resistance for both alloys is inversely related to the DR, regardless of the test environment. It is well known that subgrains or small grains can induce the activation of more slip systems due to the mutual influence of neighboring subgrains. This results in a larger degree of homogeneity of deformation. The mechanism is also confirmed by the observation of slip traces in thin foils cut from the fatigue samples with different DR. Optical microscopy showed that the frequency of occurrence of localized slip bands is greater in the large recrystallized grains than that in the unrecrystallized grains, Figure 19. Moreover, the recrystallized grains in these samples are quite large (up to 370 μm) as noted previously.

Presumably, the large grain size increases localization of strain in the slip bands which results in a high stress concentration at grain boundaries. This will result in early crack initiation by slip band decohesion, or by grain boundary cracking as exhibited in Figures 14 and 19 respectively. Subgrain boundaries also change the slip direction, thus decreasing the magnitude of localized stress and/or strain concentration. All of these factors result in a higher degree of homogeneity of deformation and a decrease in the magnitude of localized stress concentration, and improve the cyclic strain resistance for an alloy with low DR.

The magnitude of the change in cyclic strain resistance of the 1.6% Cu alloy due to the difference in DR is greater than that for the 2.1% Cu alloy, especially for tests conducted in distilled water. This effect can be attributed to the greater difference of homogeneity of deformation between the 1.6% Cu alloy with low DR and with high DR. We have shown that a sharp change in deformation behavior occurs between the 2.1% Cu alloy and the others (0.01, 1.0 and 1.6% Cu). The former alloy exhibits homogeneous cyclic deformation regardless of the magnitude of DR; thus, there is a smaller difference in degree of homogeneity of deformation due to the difference in DR, resulting in a smaller difference in the cyclic strain resistance.

The effect of DR on the LCF behavior was not determined for the low copper content alloys (0.01 and 1.0% Cu) since they did not show much difference in DR for the processing used in this study. Nevertheless, based on the results for the 1.6 and 2.1% Cu alloys and the cyclic deformation characteristics for the four different copper alloys, it would seem that the effect of DR on the LCF resistance would be more important in the low copper content alloys which exhibit more planar slip. Such an effect is in general agreement with the results of other studies[26,49], which indicate that the influence of grain size on the fatigue properties is dependent upon the slip mode.

CONCLUSIONS

1. The cyclic strain resistance of 7XXX-type aluminum alloys generally increases with increasing copper content from 0.01 to 2.1%, regardless of the test environment. Furthermore, this trend is more pronounced for tests conducted in distilled water or in a 3.5% NaCl solution. This improvement is attributed to the increased homogeneity of slip as the copper content increases.
2. The cyclic strain hardening exponents increase with increasing copper content as does the cyclic strain resistance of the alloys. This is due to the increase in copper content resulting in less shearable precipitates which increase the geometrically-necessary dislocation density.
3. For the 1.6 and 2.1% Cu alloys, the cyclic strain resistance is inversely related to the magnitude of the DR regardless of the test environment. This is attributed to a more uniform cyclic deformation of an alloy with low DR than with high DR.
4. The 2.1% Cu alloy exhibited less sensitivity to the changes in DR. This is due to a smaller difference in the homogeneity of deformation between the alloy with low DR and with high DR.
5. The environmental sensitivity of 7XXX-type alloys decreases with increasing copper content. The higher environmental sensitivity of the low copper content alloys is attributed to the fact that the localized slip bands considerably intensify the metal-environment interactions.
6. Low cycle corrosion fatigue of these alloys tested in distilled water appears to be primarily due to hydrogen embrittlement phenomenon. In a 3.5% NaCl solution, hydrogen embrittlement still plays an important role but the preferential dissolution and/or an adsorption process may also have a detrimental effect.

7. The distinct break point observed in the Coffin-Manson plots at the high plastic strain amplitude (> 1.2%) may be associated with a change in fracture mode from a brittle-like fatigue fracture at low plastic strain amplitude and/or an increase of the density and intensity of slip bands at high plastic strain amplitude.
8. The mechanisms responsible for cyclic softening can be explained in terms of the combined actions of slip-band softening and grain boundary cracking.

ACKNOWLEDGMENTS

We would like to thank Mr. H. Y. Hunsickner of the Alcoa Technical Center for suggesting this research topic and for helpful discussions during its initial stages. Numerous discussions with Drs. M. Marek, T. H. Sanders, Jr., S. B. Chakrabortty and E. E. Underwood are also gratefully acknowledged. This research was sponsored by the Air Force Office of Scientific Research, Air Force Systems Command, USAF, under Grant No. AFOSR-78-3471, Dr. Alan H. Rosenstein, Program Manager. The United States Government is authorized to reproduce and distribute reprints for Government purposes notwithstanding any copyright notation hereon.

REFERENCES

1. M. V. Hyatt and W. E. Quist, Technical Report AFML-TR-67-329, 1967, p. 827.
2. M. O. Speidel, NATO Advanced Study Institute on SCC, Copenhagen, Denmark, July, 1975.
3. R. M. N. Pelloux, Fracture, Proc. of the Second Int. Conf. on Fracture, Brighton, 1969, p. 731.
4. T. H. Sanders, Jr. and E. A. Starke, Jr., Met Trans. 7A, No. 9, 1976, p. 1407.
5. R. E. Sanders, Jr. and E. A. Starke, Jr., Met. Sci. & Eng. Vol. 28, 1977, p. 53.
6. F. S. Lin and E. A. Starke, Jr., ICF4, Waterloo, Canada, Vol. 2, 1977, p 879.
7. A. R. Rosenfield, C. W. Price and C. J. Martin, Research on Synthesis of High-Strength Al alloys, Part II, AFML-TR-74-129, 1972.
8. S. M. El-Soudani and R. M. N. Pelloux, Met. Trans. Vol. 4, 1973, p. 519.
9. C. Q. Bowles and J. Schijve, Int. J. of Fracture, Vol. 9, No. 2, 1973, p. 171.
10. W. H. Reimann and A. W. Brisbane, Eng. Fra. Mech., Vol. 5, 1973, p. 67.
11. F. Ostermann, Met. Trans., Vol. 2, 1971, p. 2897.
12. E. D. Russo, M. Conserva, F. Gatto and H. Markus, Met. Trans., Vol. 4, 1973, p. 1133.
13. J. E. Hilliard, in "Recrystallization, Grain Growth and Textures" ASM, Metal Park, Ohio, 1965, p. 267.
14. P. Cotterill and P. R. Mould, "Recrystallization and Grain Growth in Metals," A. Halsted Press Book, 1976.
15. E. A. Starke, Jr., J. of Met., Vol. 22, 1970, p. 54.
16. Y. Baba, Trans. Japan Inst. Metals, Vol. 7, 1966, p. 224.
17. C. Laird, "The General Cyclic Stress-Strain Response of Aluminum Alloys" ASTM, STP 637, 1977, p. 3.
18. G. A. Stubbington and P. J. E. Forsyth, Acta Met., Vol. 14, 1966, p. 5.
19. C. Laird and G. Thomas, Intern. J. Fracture Mech. Vol. 3, 1967, p. 81
20. C. Calabrese and C. Laird, Met. Trans., Vol. 5, 1974, p. 1785.
21. R. E. Stoltz and R. M. N. Pelloux, Met. Trans., Vol. 7A, 1976, p. 1295.

22. A. Kelly and R. B. Nicholson, Progr. Mater. Sci., Vol. 10, 1963, p. 151.

23. H. Y. Hunsicker, Aluminum, Vol. 1, ASM, Metal Park, 1967, p. 124.

24. B. W. Lifka and D. O. Sprowls, "Significance of Intergranular Corrosion in in High Strength Al Alloy Products, ASTM STP 516, 1972.

25. C. E. Feltner and C. Laird, Trans. AIME, Vol. 231, 1968, p. 1253

26. C. E. Feltner and P. Beardmore, ASTM STP 467, 1970, p. 77.

27. M. Wilhelm, M. Negeswararao and R. Meyer, to be published.

28. L. F. Coffin, Jr., J. of Materials, Vol. 6, 1971, p. 388.

29. C. Laird, V. J. Langelo, M. Hollrah, N. C. Yang, and R. de la Veaux, Dept. of Met. and Mat. Sci., U. of Penn., Philadelphia, Pa., Nov. 15, 1976.

30. R. C. Boettner, C. Laird and A. J. McEvily, Jr., Trans. AIME, Vol. 233, p. 379, 1965.

31. T. Broom and A. Nicholson, J. Inst. Metals, Vol. 89, 1960, p. 183.

32. J. A. Bennett. J. Res. of the National Bureau of Standards, Vol. 68C, 1964, p. 91.

33. R. Jacko and D. J. Duquette, Met. Trans., Vol. 8A, 1977, p. 1821.

34. C. A. Stubbington, Metallurgia, Vol. 68, 1963, p. 109.

35. R. P. Wei, Eng. Frac. Mech., Vol. 1, 1970, p. 633.

36. R. P. Wei, Int. J. of Frac. Mech., Vol. 4, 1968, p. 159.

37. E. J. Bradshaw, and C. Wheeler, Int. J. of Frac. Mech., Vol. 5, 1969, p. 255.

38. A. Hartman, Int. J. of Frac. Mech., Vol. 1, 1965, p. 167.

39. F. J. Bradshaw and C. Wheeler, Applied Mat. Res., 1966, p. 112.

40. J. A. Feeney, J. C. McMillan and R. P. Wei, Met. Trans., Vol. 1, 1970, p. 1741.

41. R. E. Stoltz and R. M. N. Pelloux, Corrosion, Vol. 29, 1973, p. 13.

42. D. J. Duquette, Corrosion Fatigue, NACE, Houston, Texas, 1972, p. 12.

43. T. Pyle, V. Rollins and D. Howard, ibid, p. 312.

44. R. E. Stoltz and R. M. N. Pelloux, Met. Trans., Vol. 3, 1972, p. 2433.

45. R. J. Jacko and D. J. Duquette, Met. Trans., Vol. 8A, 1977, p. 1821.

46. R. M. N. Pelloux, ICF2, 1969, p. 731

47. J. A. Donovan, Met. Trans., Vol. 7A, 1976, p. 1677.

48. M. R. Louthan, Jr., G. R. Caskey, Jr., J. A. Donovan and D. E. Rawl, Jr., Mater. Sci. Eng., Vol. 10, 1972, p. 317.

49. J. C. Grosskreutz, Phys. Stat. Sol. (b) Vol. 47, 1971, p. 11.

LIST OF TABLES

Table 1. Chemical Composition (Weight Percent) of the Four Aluminum Alloys.

Alloy	Cu	Zn	Mg	Zr	Ti	Fe	Si	Al
0.01 Cu	0.01	6.41	2.08	0.11	0.02	0.05	0.05	bal.
1.0 Cu	0.98	6.10	2.20	0.12	0.02	0.05	0.05	bal.
1.6 Cu	1.56	6.07	2.24	0.12	0.02	0.05	0.06	bal.
2.1 Cu	2.11	5.97	2.11	0.12	0.02	0.07	0.06	bal.

Table 2. Microstructural Parameters

Alloy	DR (volume %) L-S Section	DR (volume %) T-S Section	Subgrain Size MIL (μm)	Subgrain Size S (μm)
0.01 Cu	3	3	4.42	1.88
1.0 Cu	3	3	4.07	2.28
1.6 Cu	5	5	4.58	2.12
1.6 Cu	30	28	2.70	1.90
2.1 Cu	6	5	4.86	1.83
2.1 Cu	45	47	2.86	1.84

Table 3. Monotonic Mechanical Properties

Alloy	Yield Strength (MPa)	Tensile Strength (MPa)	Elongation (%)	Ductility (%)	n
0.01 Cu	482.2	551.7	14.0	31.2	0.028
1.0 Cu	522.3	588.0	17.1	32.5	0.031
1.6 Cu	529.2	613.5	17.9	32.5	0.033
1.6 Cu	528.2	614.7	18.7	33.1	0.030
2.1 Cu	545.9	613.5	17.1	36.4	0.032
2.1 Cu	533.1	615.4	17.3	35.3	0.033

Table 4. The LCF Data Tests Conducted in Dry Air, Distilled Water and a 3.5% NaCl Solution.

Alloy	DR (volume %)	Dry Air -C	Dry Air $2N_f = 1$	Dry Air n'	H_2O -C	H_2O $2N_f = 1$	H_2O n'	3.5% NaCl -C	3.5% NaCl $2N_f = 1$	3.5% NaCl n'
0.01 Cu	3	0.82 0.43	125 16	0.063	0.68	23	0.063	0.68	20	0.063
1.0 Cu	3	0.78 0.48	115	0.075	0.77	63	0.075	-	-	-
1.6 Cu	5	0.77 0.48	110 24	0.088	0.85 0.43	125 19	0.088	0.85 0.54	100 16	0.088
1.6 Cu	30	0.79 0.51	118 24	0.082	0.93 0.42	180 13	0.082	0.85	90	0.082
2.1 Cu	6	0.63	46	0.114	0.68 0.41	54 14	0.114	0.70	62	0.114
2.1 Cu	45	0.67 0.43	50 20	0.099	0.71 0.48	60 20	0.099	-	-	-

LIST OF FIGURES

Figure 14. Observation of slip band cracks on the polished surfaces of the LCF samples tested in dry air before failure, (a) the 0.01% Cu alloy with 3% DR, $\Delta\varepsilon_p/2$ = 0.72% for 80 cycles, and (b) the 1.6% Cu alloy with 5% DR, $\Delta\varepsilon_p/2$ = 0.81% for 100 cycles.

Figure 15. Scanning electron fractographs of the fatigue fracture surfaces for the 1.6% Cu alloy with 30% DR tested in dry air, (a) the plastic strain amplitude below the break point, $\Delta\varepsilon_p/2$ = 0.11%, N_f = 2090 cycles. (b) above the break point, $\Delta\varepsilon_p/2$ = 2.61%, N_f = 22 cycles.

Figure 16. Effect of environments on the LCF behavior of (a) the 0.01% Cu alloy with 3% DR, (b) the 1.0% Cu alloy with 3% DR, (c) the 1.6% Cu alloy, and (d) the 2.1% Cu alloy.

Figure 17. Scanning electron fractographs of the fatigue fracture surfaces for the 0.01% Cu alloy tested in various environments, (a) in dry air, $\Delta\varepsilon_p/2$ = 0.34%, N_f = 384 cycles, (b) in distilled water, $\Delta\varepsilon_p/2$ = 0.18%, N_f = 342 cycles. Arrow indicates direction of the crack propagation.

Figure 18. Scanning electron fractographs of the fatigue fracture surfaces for the 2.1% Cu alloy with 6% DR tested in various environments, (a) in dry air, $\Delta\varepsilon_p/2$ = 0.18%, N_f = 1562 cycles, (b) in distilled water, $\Delta\varepsilon_p/2$ = 0.18%, N_f = 1054 cycles.

Figure 19. Observation of the polished surfaces of the LCF samples for the 1.6% Cu alloy with 30% DR tested in dry air for 60 cycles, (a) $\Delta\varepsilon_p/2$ = 0.78%, showing PSB's and grain boundary cracking in the recrystallized grains, (b) $\Delta\varepsilon_p/2$ = 0.67%, showing PSB's in the recrystallized grains. HNO_3 etch.

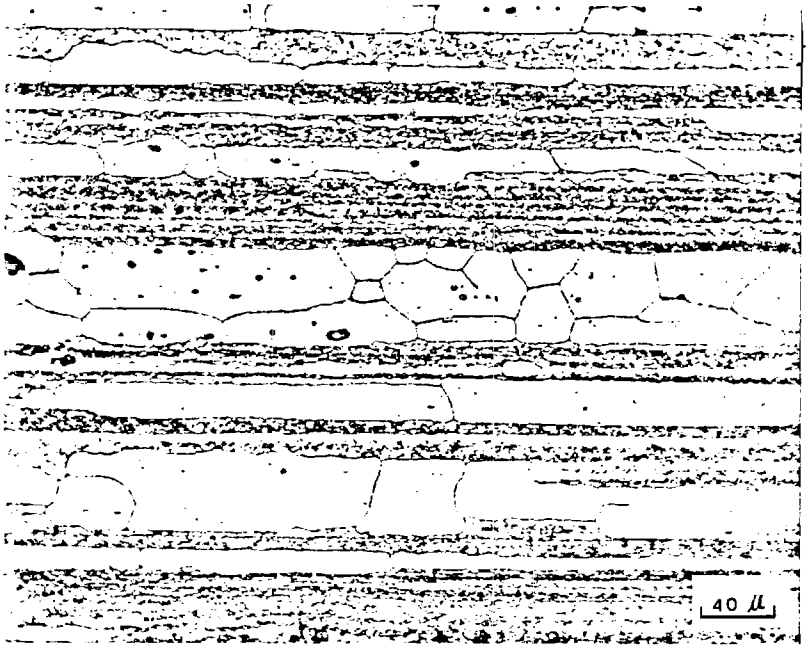

(A)

(B)

Figure 1. (a) Microstructure of the 2.1% Cu alloy with 45% DR, (b) microstructure of the 0.01% Cu alloy with 3% DR; HNO_3 etch.

(A)

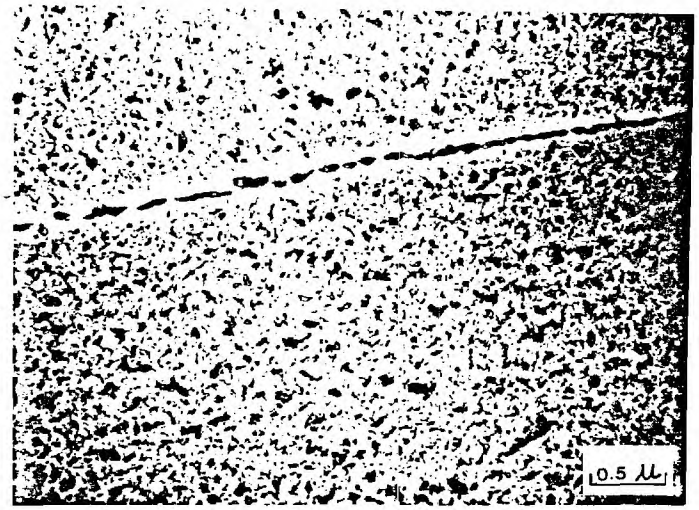

(B)

Figure 2. Transmission electron micrographs of precipitation features of the 2.1% Cu alloy, (a) subgrain boundaries, and (b) a high angle grain boundary.

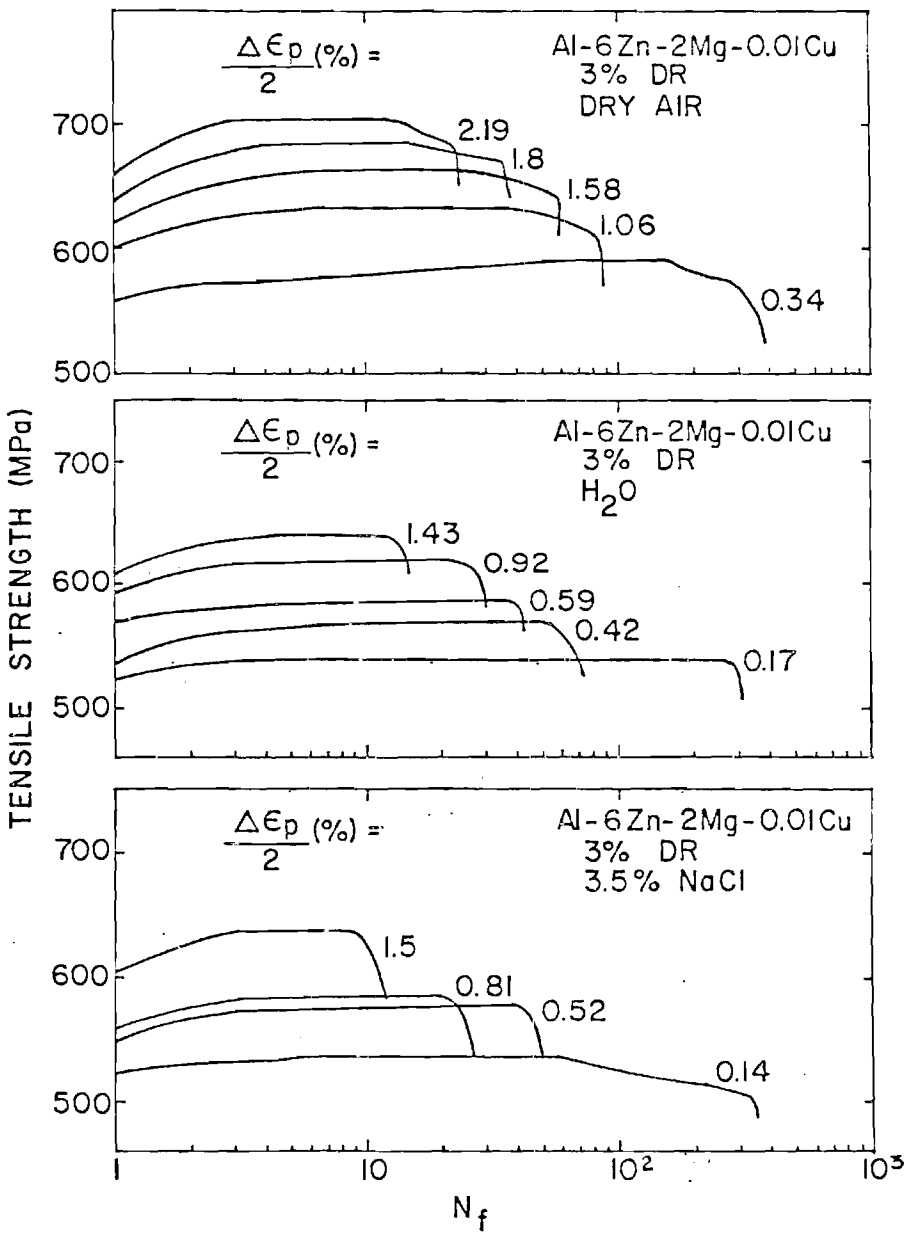

Figure 3. Cyclic hardening and softening curves for the 0.01% Cu alloy tested in various environments.

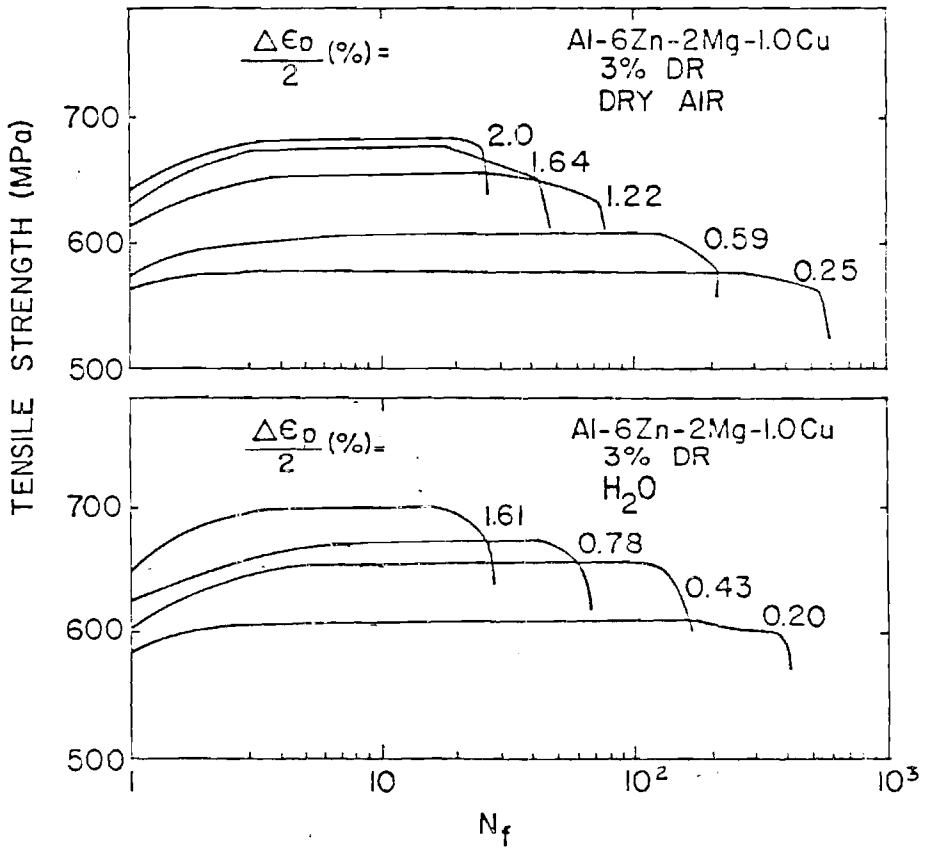

Figure 4. Cyclic hardening and softening curves for the 1.0% Cu alloy tested in dry air and distilled water.

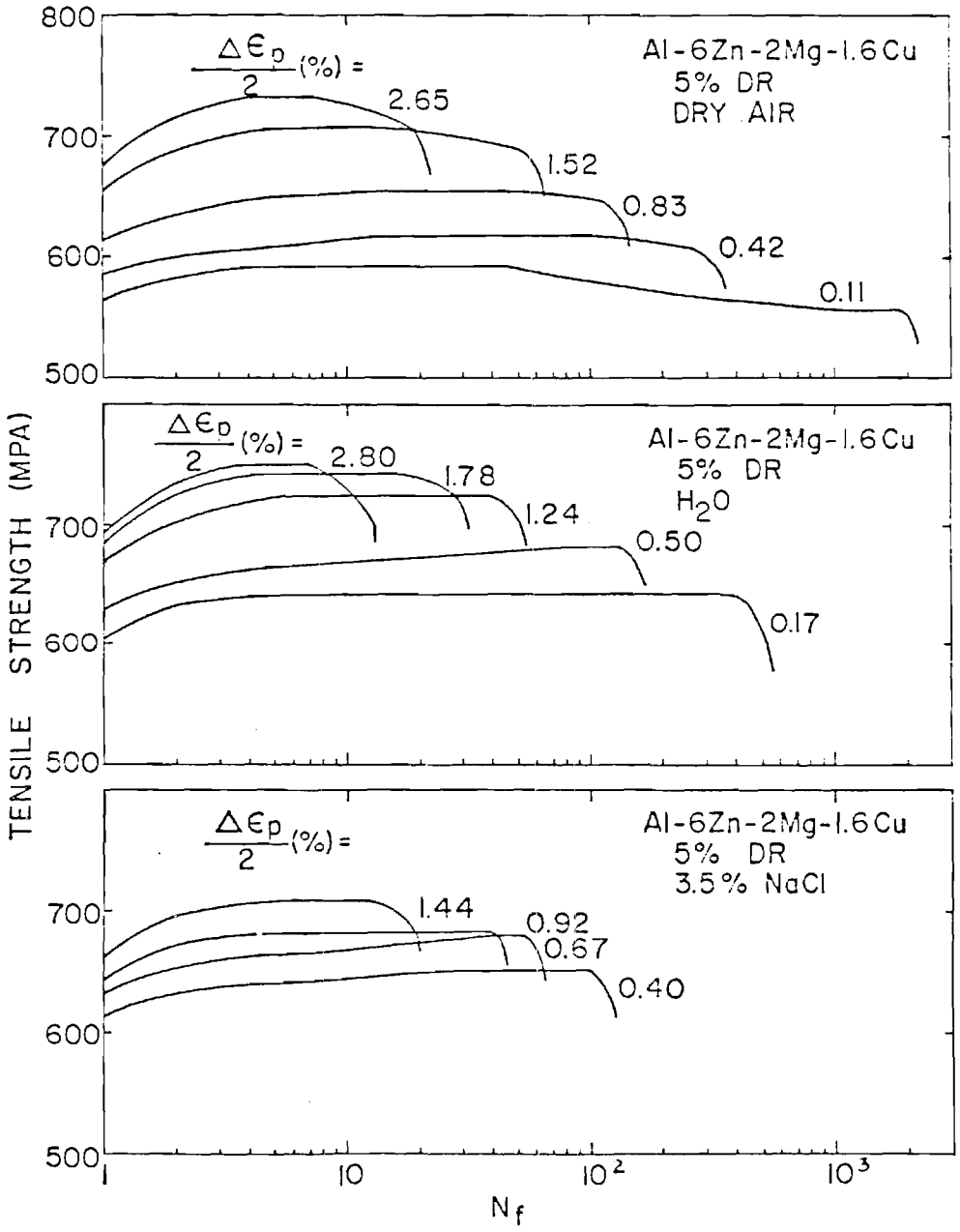

Figure 5. Cyclic hardening and softening curves for the 1.6% Cu alloy with 5% DR tested in various envirnoments.

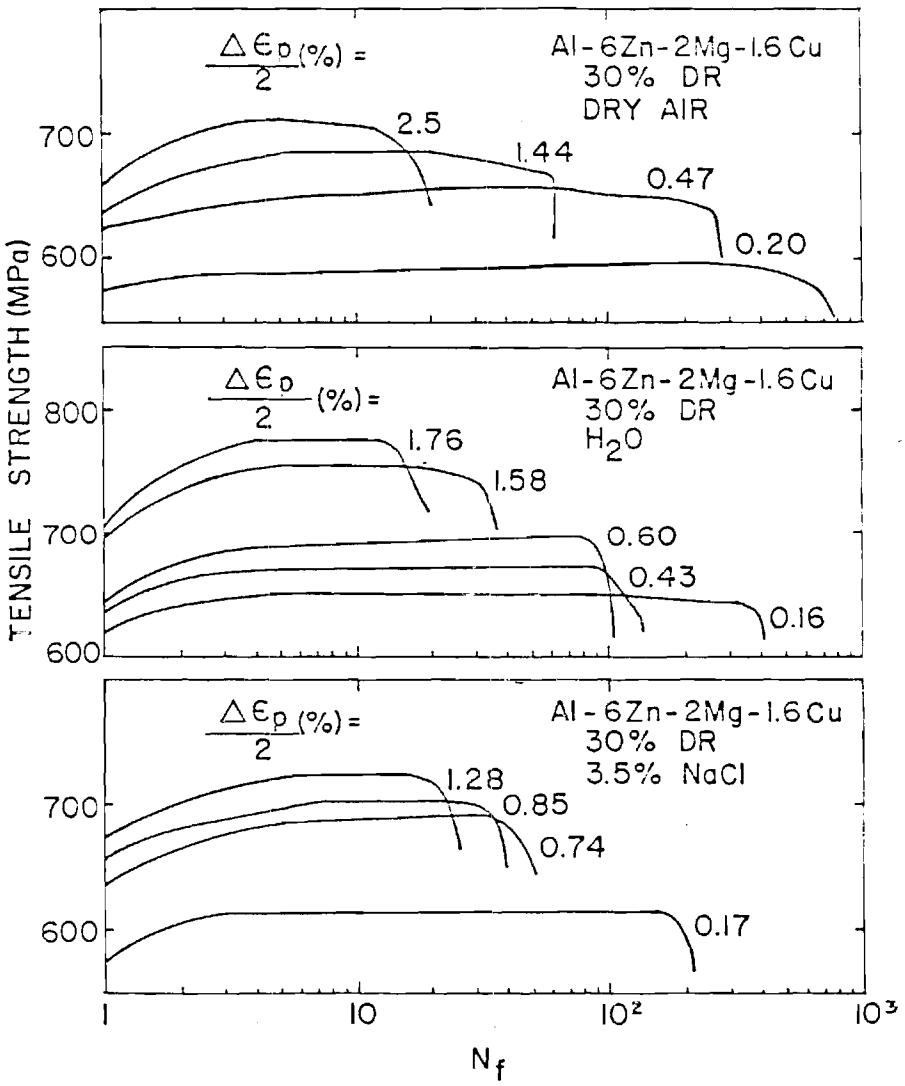

Figure 6. Cyclic hardening and softening curves for the 1.6% Cu alloy with 30% DR tested in various environments.

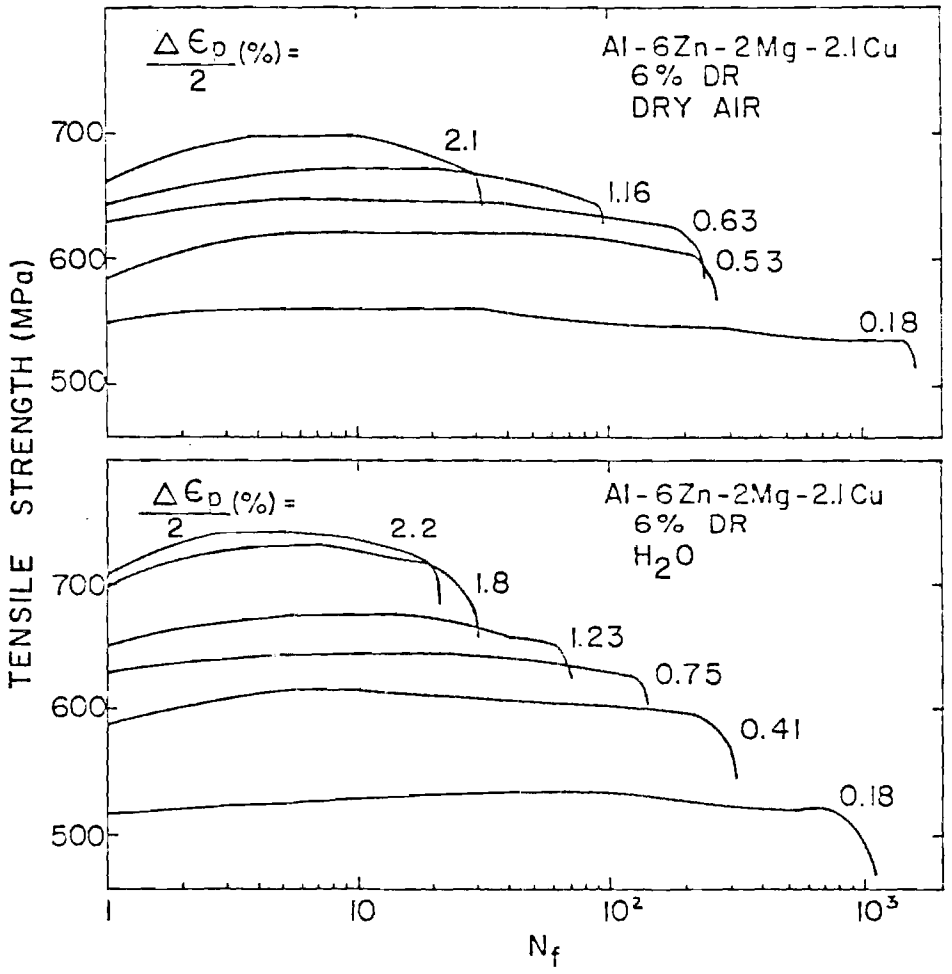

Figure 7. Cyclic hardening and softening curves for the 2.1% Cu alloy with 6% DR tested in dry air and distilled water.

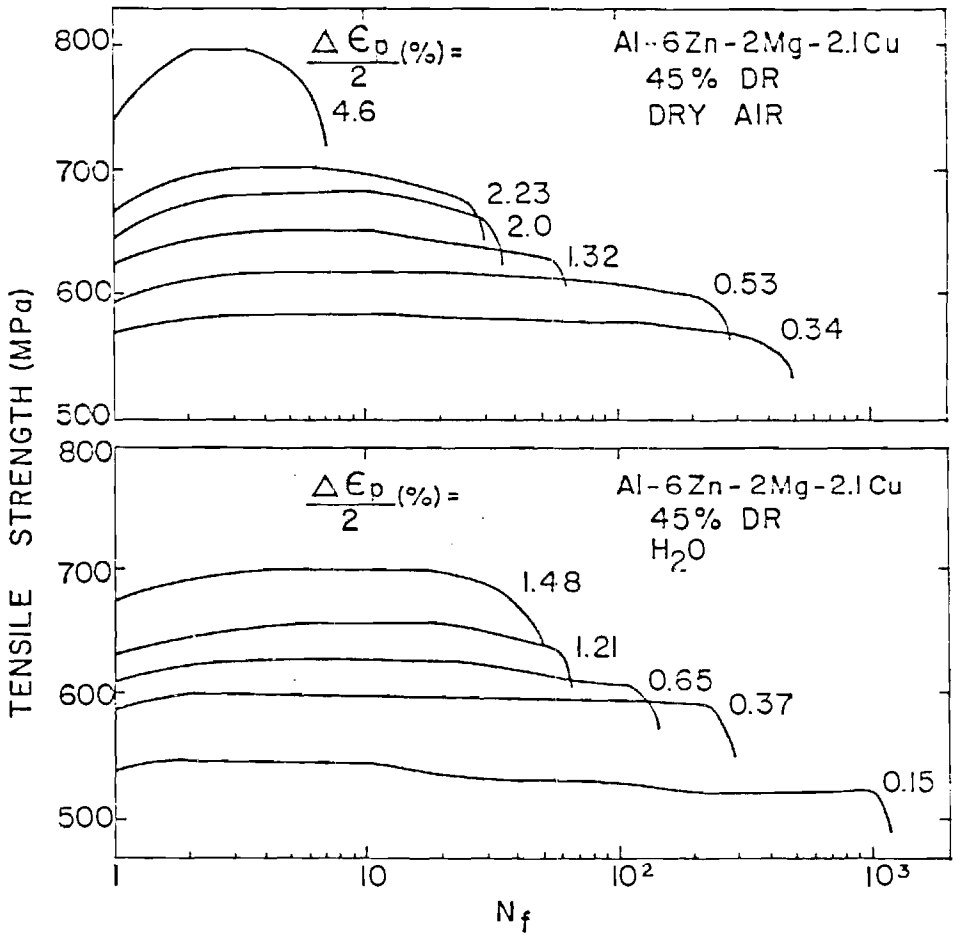

Figure 8. Cyclic hardening and softening curves for the 2.1% Cu alloy with 45% DR tested in dry air and distilled water.

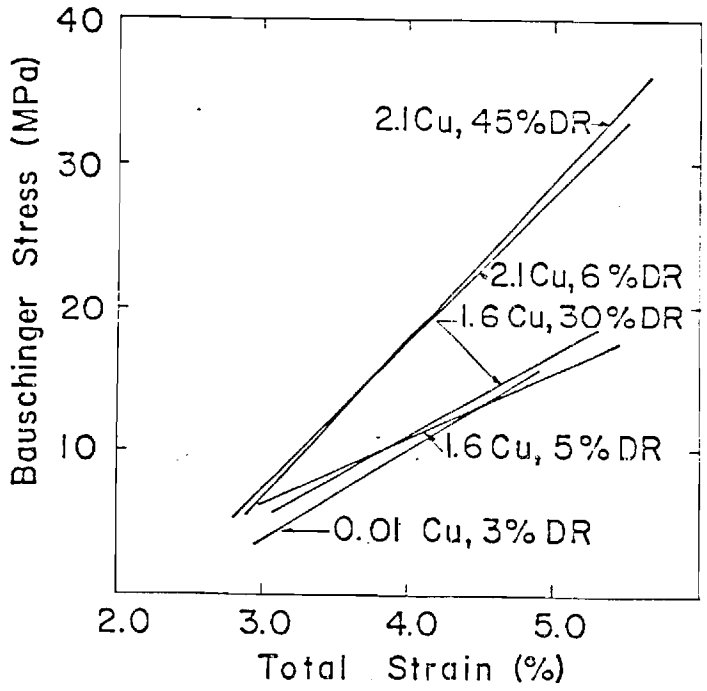

Figure 9. The effect of copper content in 7XXX-type aluminum alloys on the Bauschinger effect at the first half cycle.

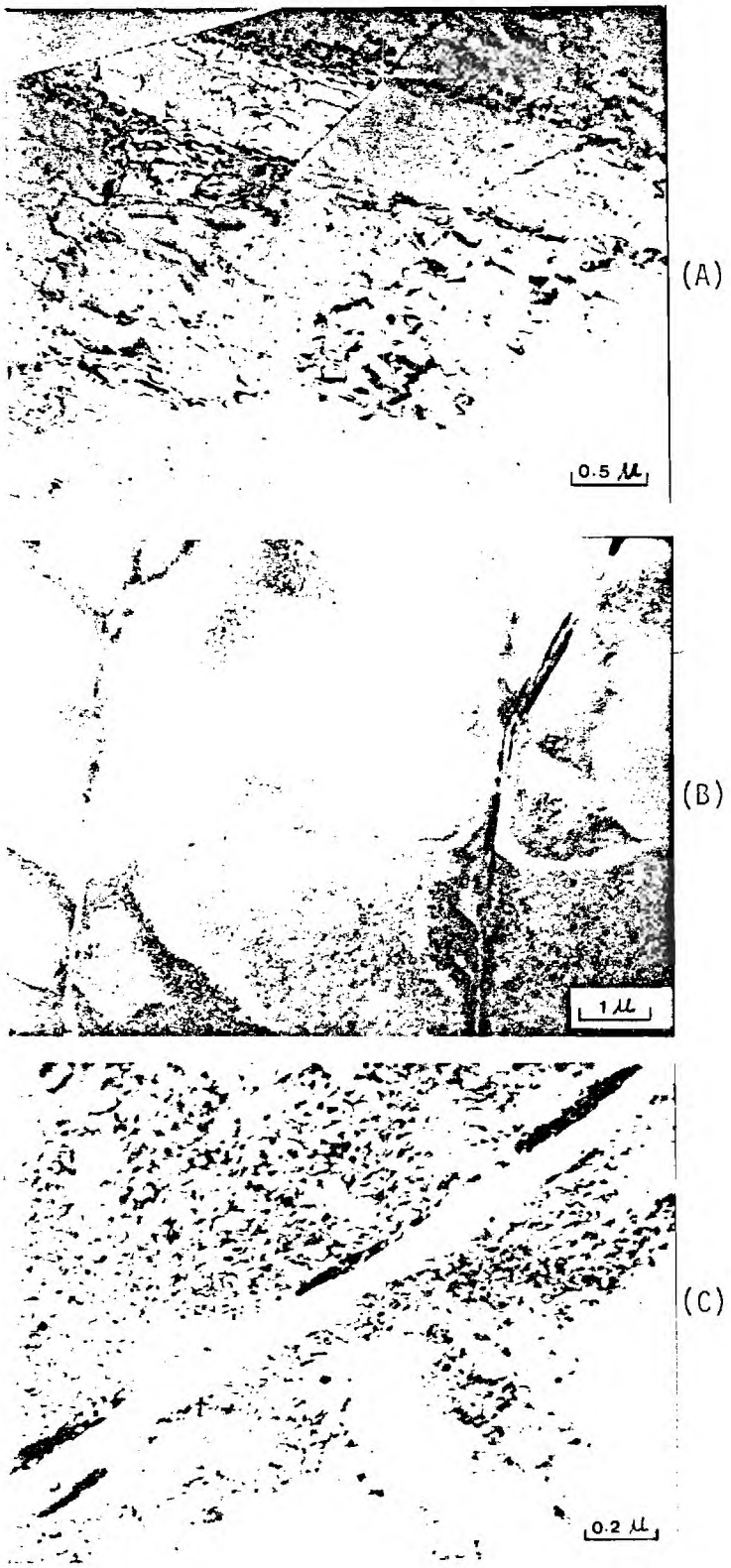

Figure 10. Transmission electron micrographs of the LCF samples for the 0.01% Cu alloy with 3% DR tested in dry air until failure, showing slip bands. (a) plastic strain amplitude, $\Delta\varepsilon_p/2 = 0.53\%$, $N_f = 215$ cycles, slip band is parallel to [011], (b) $\Delta\varepsilon_p/2 = 2.2\%$, $N_f = 24$ cycles, and (c) high mag. of (b), slip band is parallel to [101].

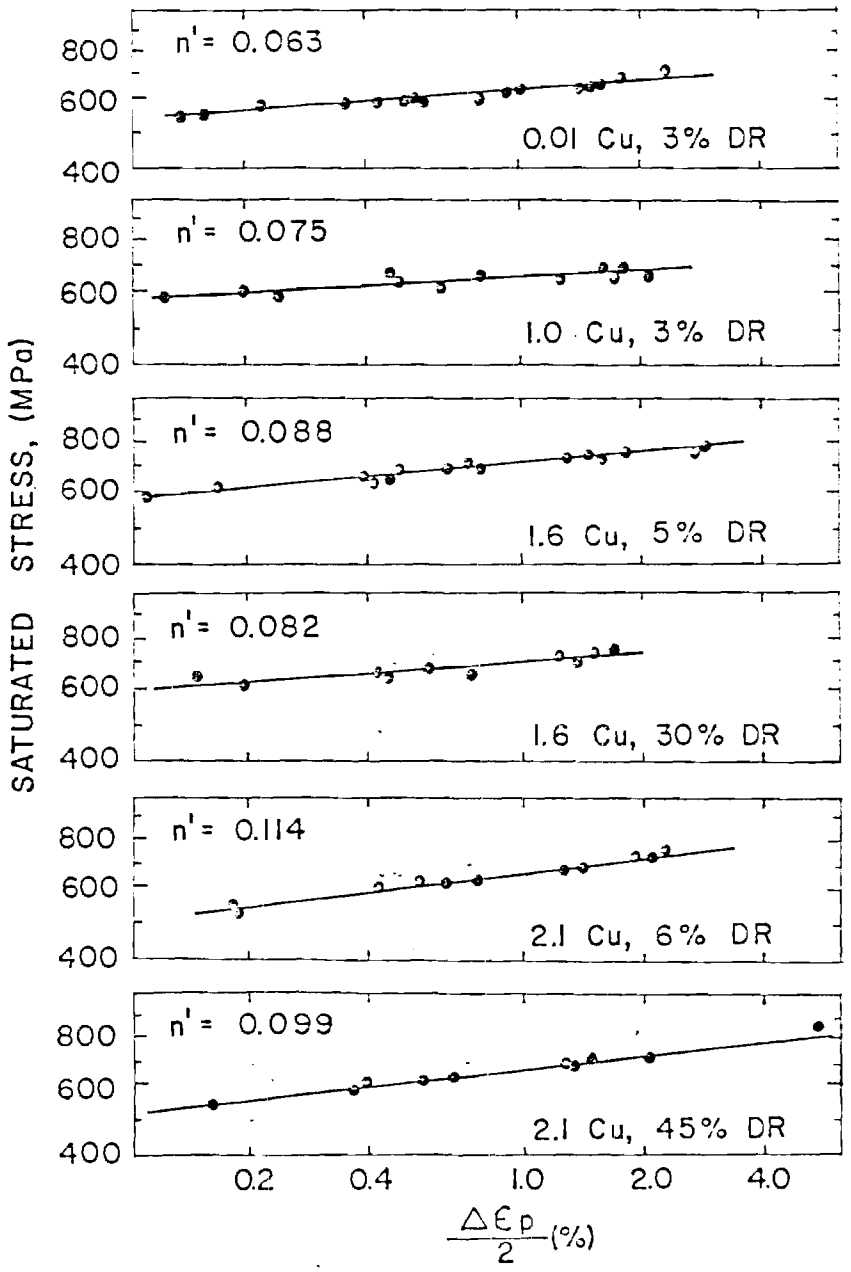

Figure 11. Cyclic stress-strain curves for various Al-6Zn-2Mg-xCu aluminum alloys.

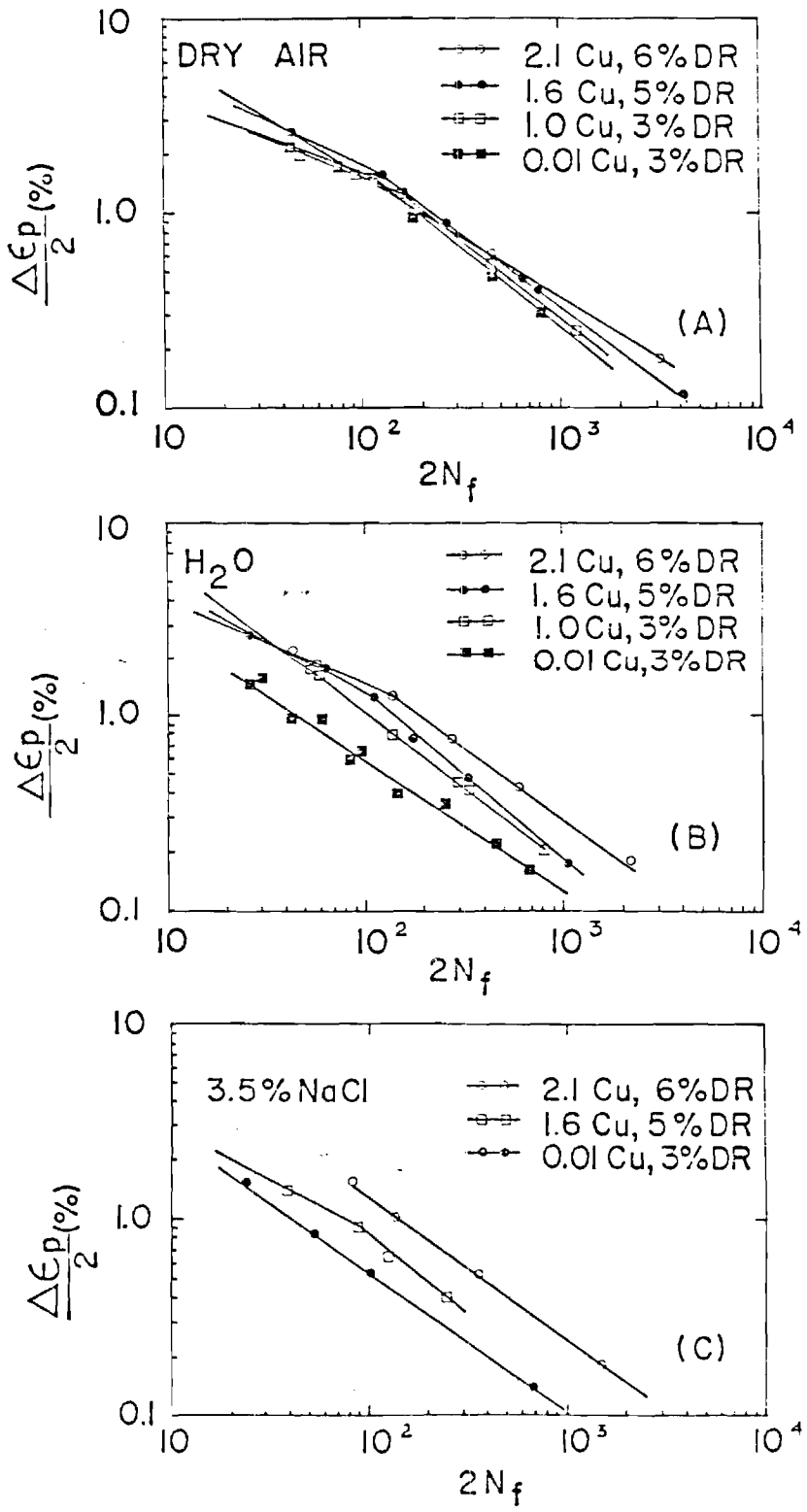

Figure 12. Effect of the copper content of 7XXX-type aluminum alloys of the LCF behavior, tests conducted in (a) dry air, (b) distilled water and (c) a 3.5% NaCl solution.

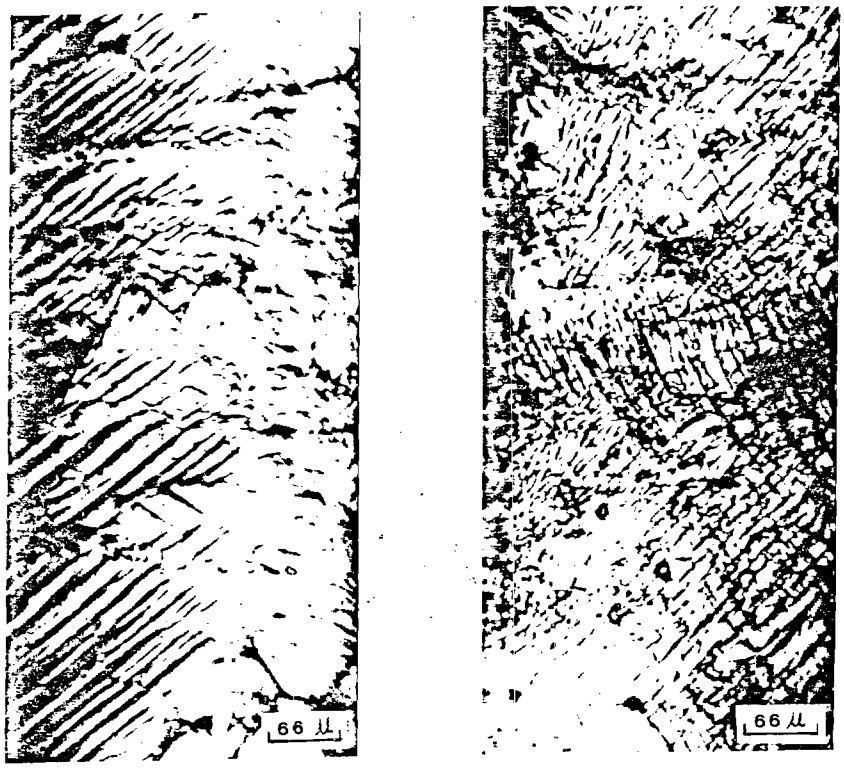

(A) (B)

Figure 13. Observations of slip traces on the polished surfaces of the LCF samples tested in dry air for 80 cycles, (a) the 0.01% Cu alloy with 3% DR, $\Delta\varepsilon_p/2$ = 0.72%, and (b) the 2.1% Cu alloy with 6% DR, $\Delta\varepsilon_p/2$ = 0.76%. Loading axis was vertical.

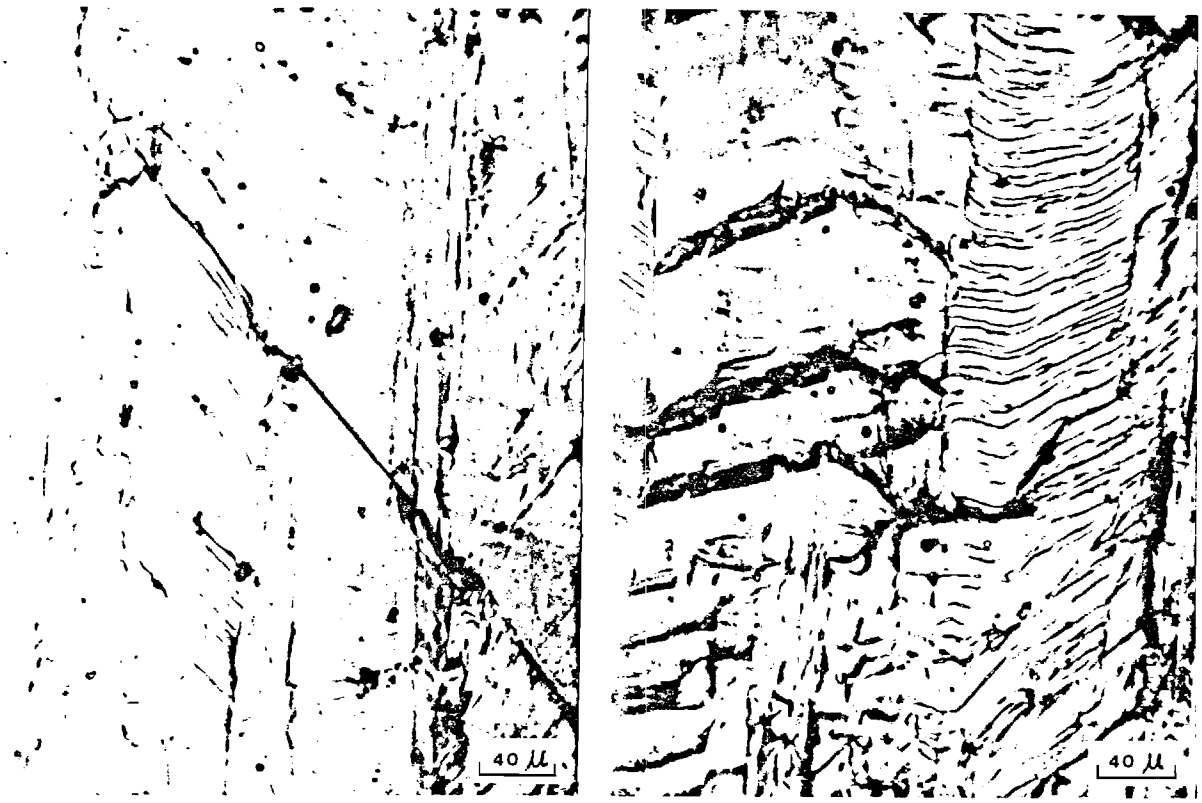

Figure 14. Observation of slip band cracks on the polished surfaces of the LCF samples tested in dry air before failure, (a) the 0.01% Cu alloy with 3% DR, $\Delta\varepsilon_p/2$ = 0.72% for 80 cycles, and (b) the 1.6% Cu alloy with 5% DR, $\Delta\varepsilon_p/2$ = 0.81% for 100 cycles.

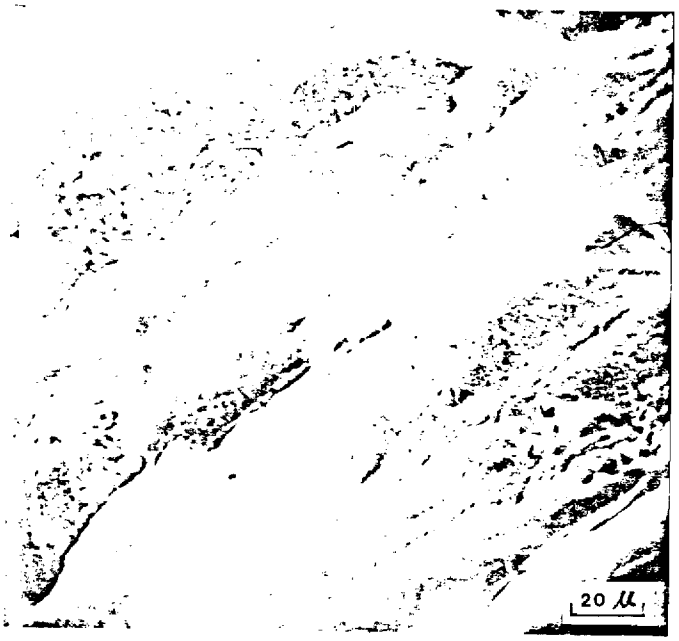

(A)

(B)

Figure 15. Scanning electron fractographs of the fatigue fracture surfaces for the 1.6% Cu alloy with 30% DR tested in dry air, (a) the plastic strain amplitude below the break point, $\Delta\varepsilon_p/2 = 0.11\%$, $N_f = 2090$ cycles. (b) above the break point, $\Delta\varepsilon_p/2 = 2.61\%$, $N_f = 22$ cycles.

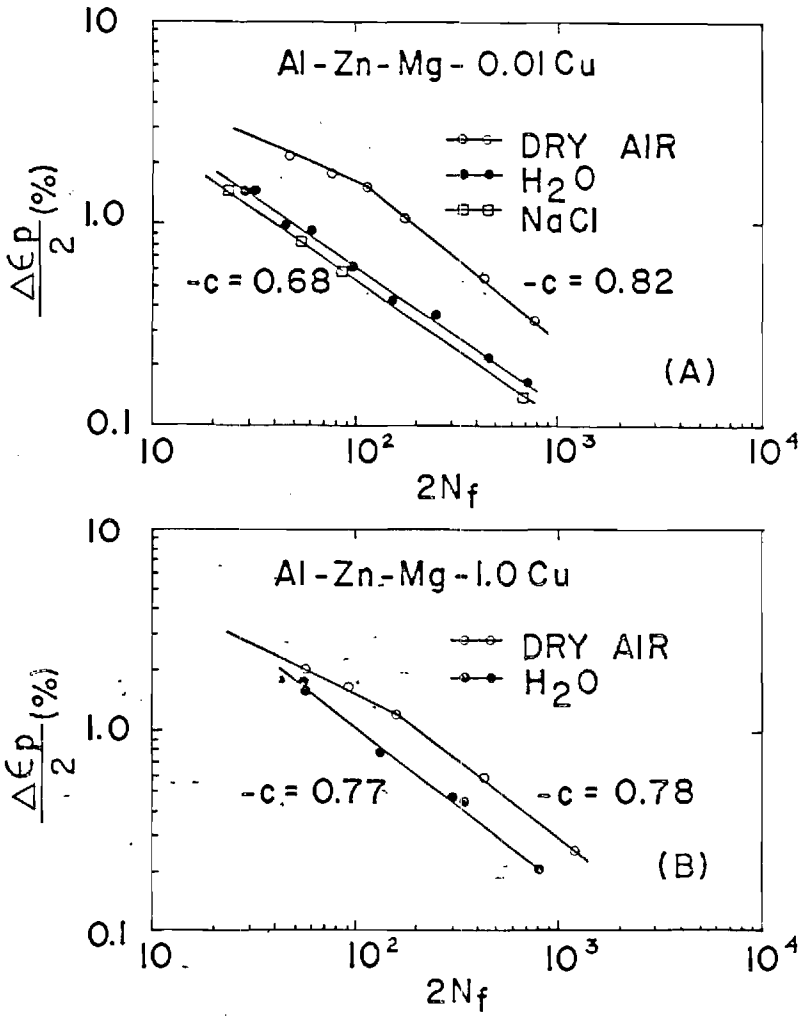

Figure 16. Effect of environments on the LCF behavior of (a) the 0.01% Cu alloy with 3% DR, (b) the 1.0% Cu alloy with 3% DR, (c) the 1.6% Cu alloy, and (d) the 2.1% Cu alloy.

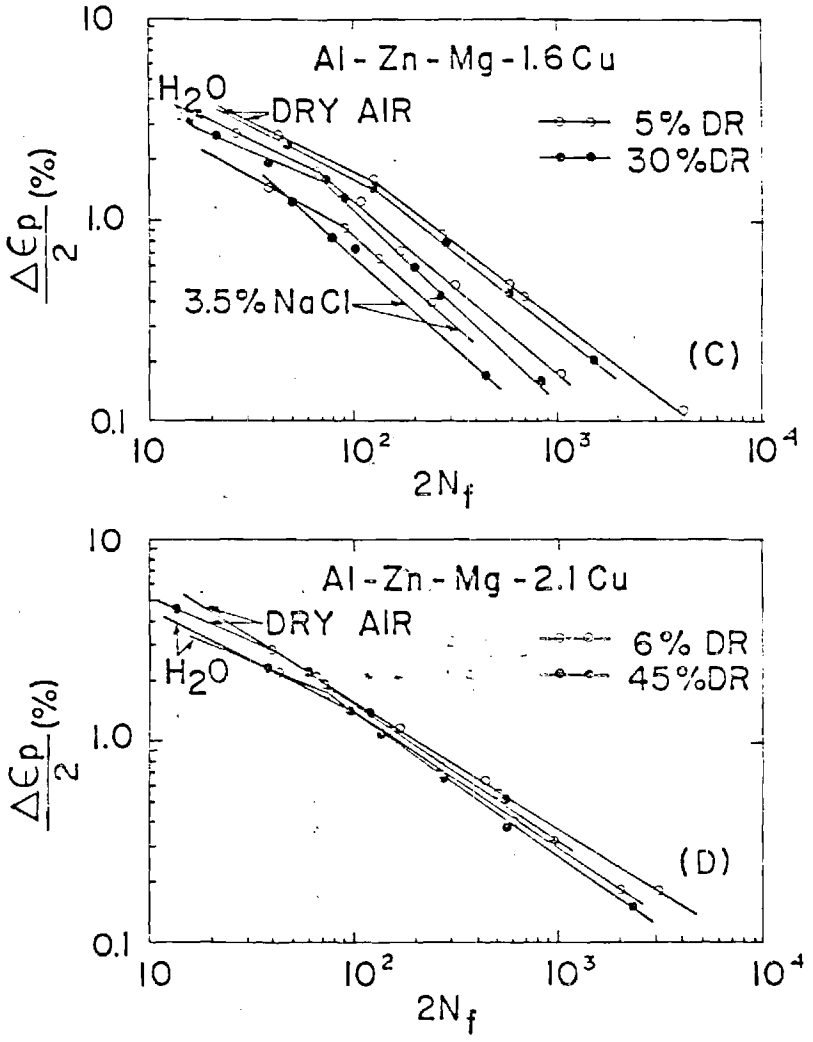
Al - Zn - Mg - 1.6 Cu
H_2O
DRY AIR
5% DR
30% DR
3.5% NaCl
(C)
$\frac{\Delta \epsilon p}{2}$ (%)
10
1.0
0.1
10
10^2
10^3
10^4
$2N_f$
Al - Zn - Mg - 2.1 Cu
DRY AIR
H_2O
6% DR
45% DR
(D)
$\frac{\Delta \epsilon p}{2}$ (%)
10
1.0
0.1
10
10^2
10^3
10^4
$2N_f$

(A)

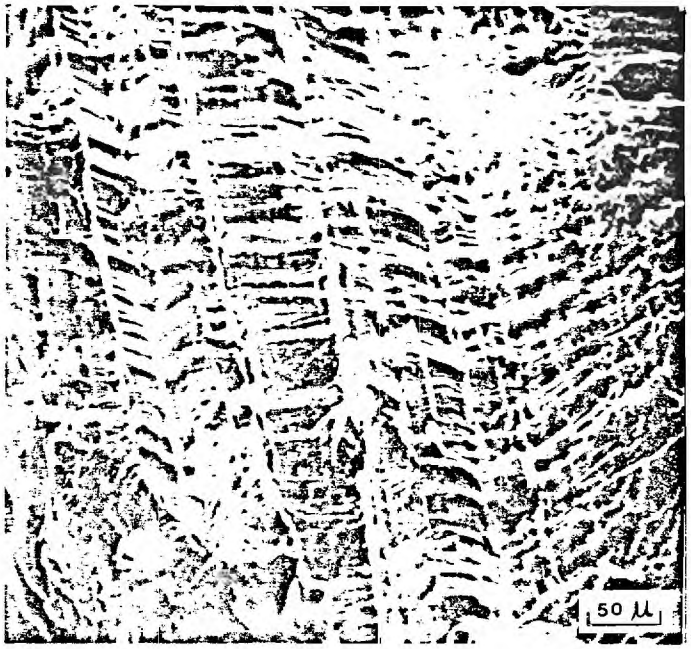

(B)

Figure 17. Scanning electron fractographs of the fatigue fracture surfaces for the 0.01% Cu alloy tested in various environments, (a) in dry air, $\Delta\varepsilon_p/2 = 0.34\%$, $N_f = 384$ cycles, (b) in distilled water, $\Delta\varepsilon_p/2 = 0.18\%$, $N_f = 342$ cycles. Arrow indicates direction of the crack propagation.

(A)

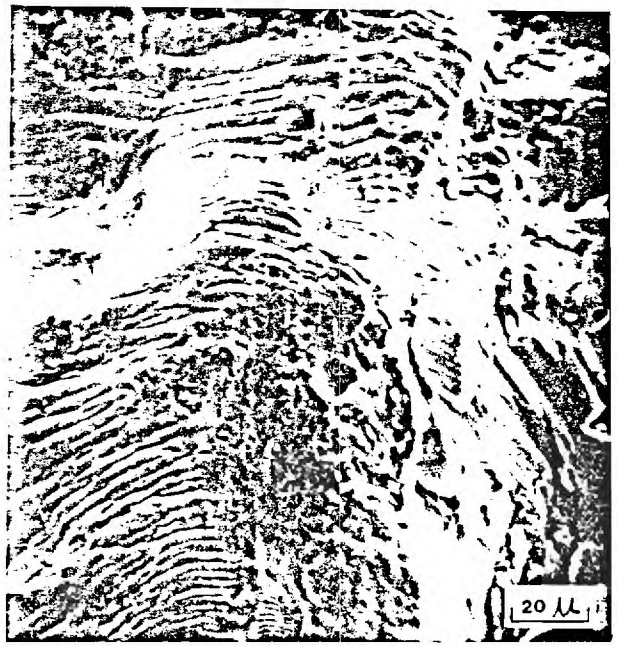

(B)

Figure 18. Scanning electron fractographs of the fatigue fracture surfaces for the 2.1% Cu alloy with 6% DR tested in various environments, (a) in dry air, $\Delta\varepsilon_p/2 = 0.18\%$, $N_f = 1562$ cycles, (b) in distilled water, $\Delta\varepsilon_p/2 = 0.18\%$, $N_f = 1054$ cycles.

(A)

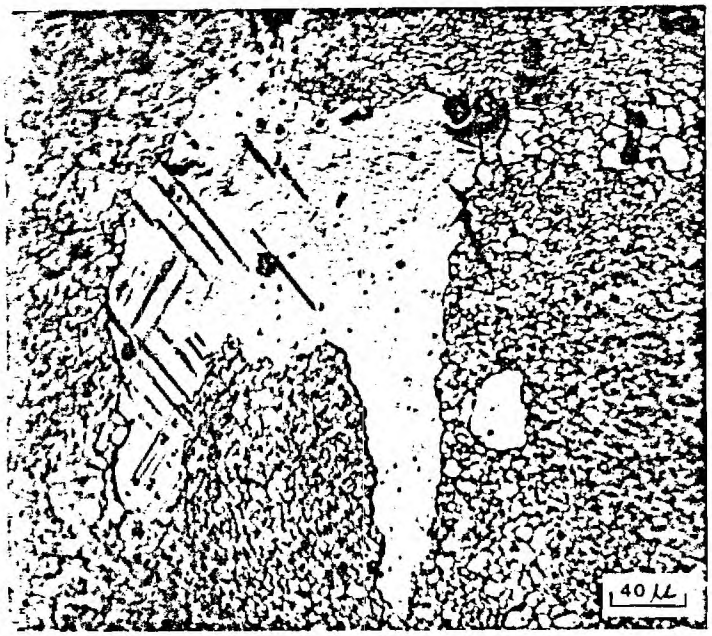

(B)

Figure 19. Observation of the polished surfaces of the LCF samples for the 1.6% Cu alloy with 30% DR tested in dry air for 60 cycles, (a) $\Delta\varepsilon_p/2 = 0.78\%$, showing PSB's and grain boundary cracking in the recrystallized grains, (b) $\Delta\varepsilon_p/2 = 0.67\%$, showing PSB's in the recrystallized grains. HNO_3 etch.